Bulletin of Faculty of Science, Zagazig University (BFSZU)
e-ISSN: 1110-1555
Volume-2024, Issue-3, pp-6-30
https://bfszu.journals.ekb.eg/journal
Research Paper DOI: 10.21608/bfszu.2023.241229.1324

==========

Petrophysical evaluation of the turbidite channels in Kafr Elsheikh Formation using wireline logging, West El-Burullus gas field, Offshore Nile Delta, Egypt

Ashraf Ghoneimi [1], Muhammad Nabih [1], Mahmoud El-Sadany [2], Ahmed H. Saleh [1]

[1]Geology Department, Faculty of Science, Zagazig University, Zagazig, 44519, Egypt.
[2] Exploration Department, Egyptian Natural Gas Holding Company (EGAS), Egypt.
Corresponding author: Mahmoud El-Sadany [2] Email: masadany0@gmail.com

***ABSTRACT*: West El-Burullus area reflected complicated reservoirs consisting of turbidite channels system of the Pliocene shales intercalated with sands forming the Kafr El-Sheikh Formation (FM.). Such turbidites represent a great challenge in accurately determining the existence of hydrocarbons, we have adopted a specific petrophysical evaluation technique using well-logging properties integrated with the modular dynamic formation tester (MDT) followed by Cross-plotting relationships as lithological/hydrocarbon identification. West El Burullus area, it's proved that have two fields, namely Web and Papyrus fields. Kafr El-Sheikh FM. Three wells (WEB-1, Bamboo-1, and Papyrus-1) are chosen to evaluate the hydrocarbon occurrence in Kafr El-Sheikh FM. WEB-1 and Bamboo-1 well targeted the same reservoir (Web), while the Papyrus-1 well targeted another reservoir (Papyrus). The results proved that Kafr Elsheikh FM. in the wells (Web-1and Papyrus-1) wells contains hydrocarbon with an average net pay of around 16.8m and 15.14m respectively; On the other hand, the Bamboo-1 well does not contain any hydrocarbon that reflects the failure of the well by entering outside the boundaries of the Web Reservoir. All results are matched with MDT. For the Web reservoir, from the MDT plot the water gradient values range from 0.427 psi/ft to 0.448 psi/ft, and the gas gradient value is 0.119 psi/ft. Also for the Papyrus reservoir, the gas gradient values range from 0.099 psi/ft and 0.212 psi/ft as condensate for two different zones. Those types of gases are likely rich gas and thermogenic (may be Miocene sourced) migrated through major faults such as Rashid fault and its successive faults.**

***KEYWORDS:* West El Burullus; Nile Delta; Kafr El-Sheikh FM; Petrophysical evaluation; Turbidites; MDT.**

Date of Submission: 09-10-2023 Date of acceptance: 23-11-2023

I. INTRODUCTION

The Pliocene Sediments of the Kafr El Sheikh Formation represents a gas reservoir in West El-Burullus (WEB) gas discovery field in the Mediterranean Sea, western Nile Delta (ND) offshore basin, south from west Delta deep marine (WDDM) area. It lies between latitudes 31° 30` 50" and 31° 38` 30"N and longitudes 30° 21` 35" and 30° 31` 20" E approximately (Fig. 1). Two fields are discovered through the WEB-1 and Papyrus-1 wells in the WEB area. This study relies heavily on Petrophysical analysis for three wells (WEB-1, Bamboo-1, and Papyrus-1) with different aspects depending on the available logging data. That has been a worthy successor in fluvial-deltaic and basin floor turbidite-fan systems because it is a powerful tool for the analysis of delineating subtle stratigraphic plays such as channels, overbank, levees, and fan deposits. Petrophysics concentrates on calculating porosity and fluid saturation as a function of depth in a well. Then using the modular dynamic formation tester (MDT) to confirm the interpretation of the logs, followed by Cross-plotting relationships as lithological/hydrocarbon identification.

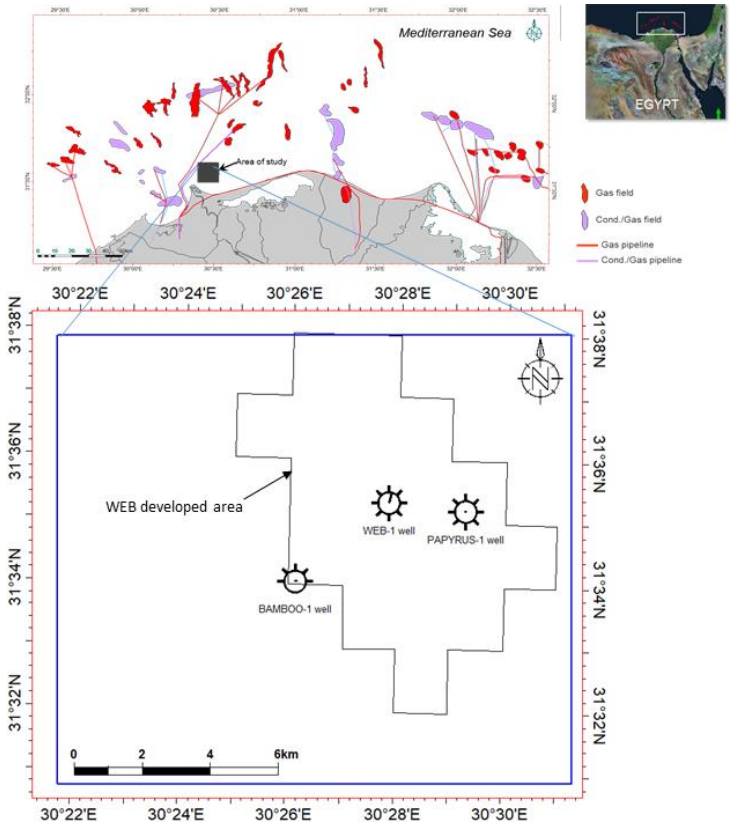

Figure 1: The location map of the West El-Burullus area shows the seismic survey coverage and well location.

GEOLOGIC SETTING

Three central petroleum provinces divided Egypt into the Gulf of Suez, the ND, and the Western Desert. Three major structural features of a triangular megastructure characterize the offshore ND. In the south, the Delta is restricted by an E-W trending fault named the Hinge line as a paleo passive margin, which separates the continental shelf to the south destination from the ND sedimentation system to the north [1]. The western ND is cut across by a significant slip fault striking NE-SW direction, namely the Rosetta fault as a paleo transform fault. It splits the West El-Burullus concession into two uneven areas, Burullus high to the southeast. At the same time, at the northwest, a big half-graben has a regional dip to the southeast with a crest lying on ND offshore anticline (Fig. 2a) [2]. The eastern ND is cut across by a major NW-SE strike-slip fault, the Temsah fault, as a paleo-rifting system, representing the Rosetta fault's counterpart. Its hanging wall shows a prolific series of parallel tilted fault blocks [3].

The West El-Burullus area is located on the Burullus horst block dipping to the north and limited towards the northwest by the regional Rosetta fault and towards the southeast by the Burullus normal fault. Both regional faults are oriented NE-SW (Fig. 2a). The Burullus regional high is displayed with the WEB reservoir put in the Pliocene slope settings of the Delta (Fig. 2b) [4]. The faults are thought to provide an active structural control o during the deposition of the sediments throughout the Pliocene time. The horst is faulted by minor normal faults (Fig. 2a and b). Growth faults have induced syn-sedimentary faults by gravity and compaction of the sediments, creating local topography and accommodation for ponded turbidites during the depositional history. Many authors [5-6-7] discussed ND Pliocene stratigraphy. The Late Miocene-Early Pliocene Rosetta anhydrite is environmentally deposited in a sabkha condition. The Rosetta FM is overlain by Abu Madi FM, which complies with fluvial-deltaic deposition to marine coastal sedimentation, generally deposited in SSE-NNW trending valleys. It is a fining-up FM composed of quartzose sands, infrequent conglomerates later becoming dominated by increasing clay interbeds towards the maximum flooding surface at the base of Pliocene. Otherwise, the lower-middle Pliocene sediments of Kafr El-Sheikh FM correspond to deep water sediments deposited in outer shelf or slope environments related to the study area (Fig. 2b) [4].

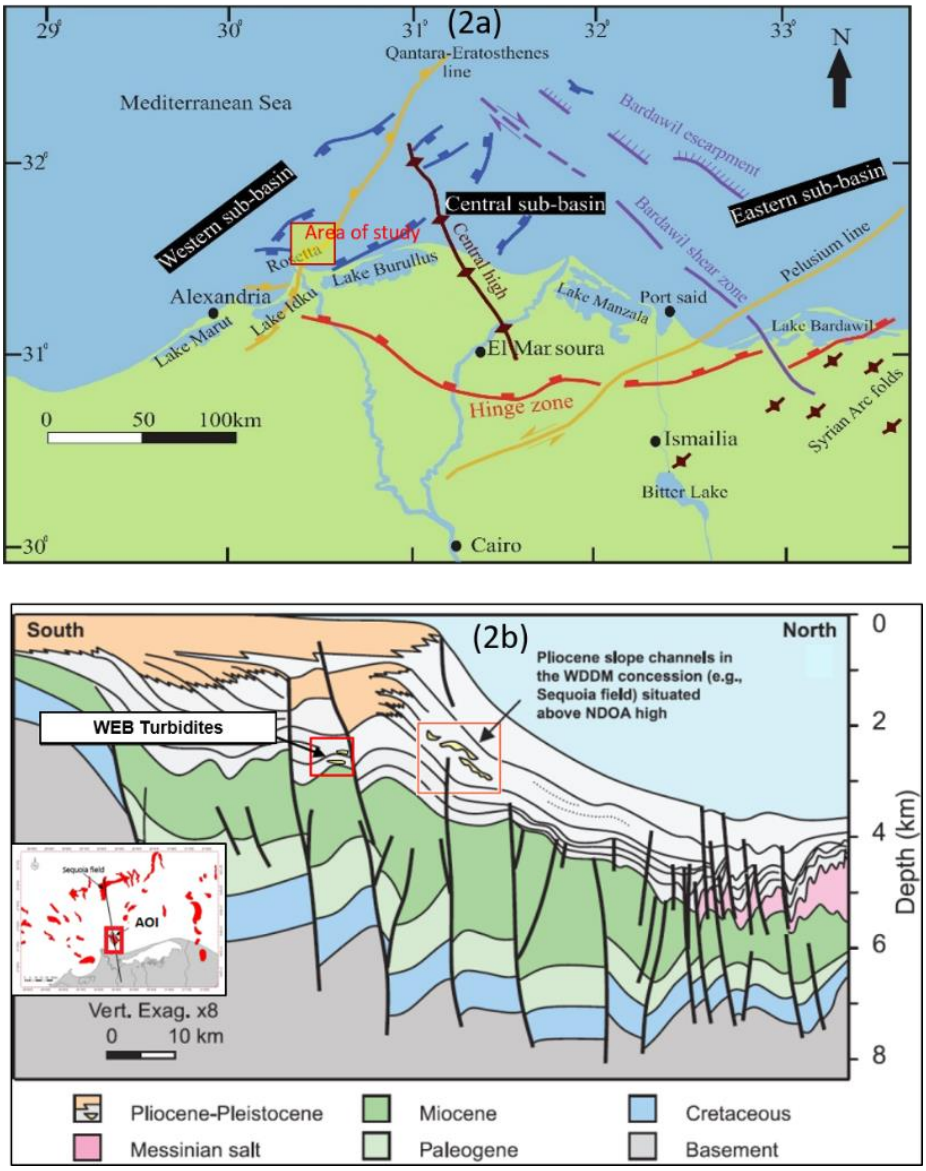

Figure 2: (a) Structural pattern of North ND sub-basins [2], and (b) Regional geological cross-section shows the tectonic framework and the stratigraphic aspects affecting the study area [4].

It comprises silts and muds with infrequent thin interbedded sands (turbidites). Kafr El-Sheikh FM is of Lower-Middle Pliocene age and comprises deep water sediments deposited in outer shelf and slope environments. It consists of muds and silts with occasional thin interbedded sands. The general ND stratigraphic column with WEB reservoir from logging is shown in (Fig. 3) [8]. It comprises sediments of the Miocene to the Holocene age. This sequence is a thick pile of clastic sediments in which the West El-Burullus discovery has been made. The sand reservoirs of these fields are of the middle Pliocene age and form part of the Kafr El-Sheikh FM.

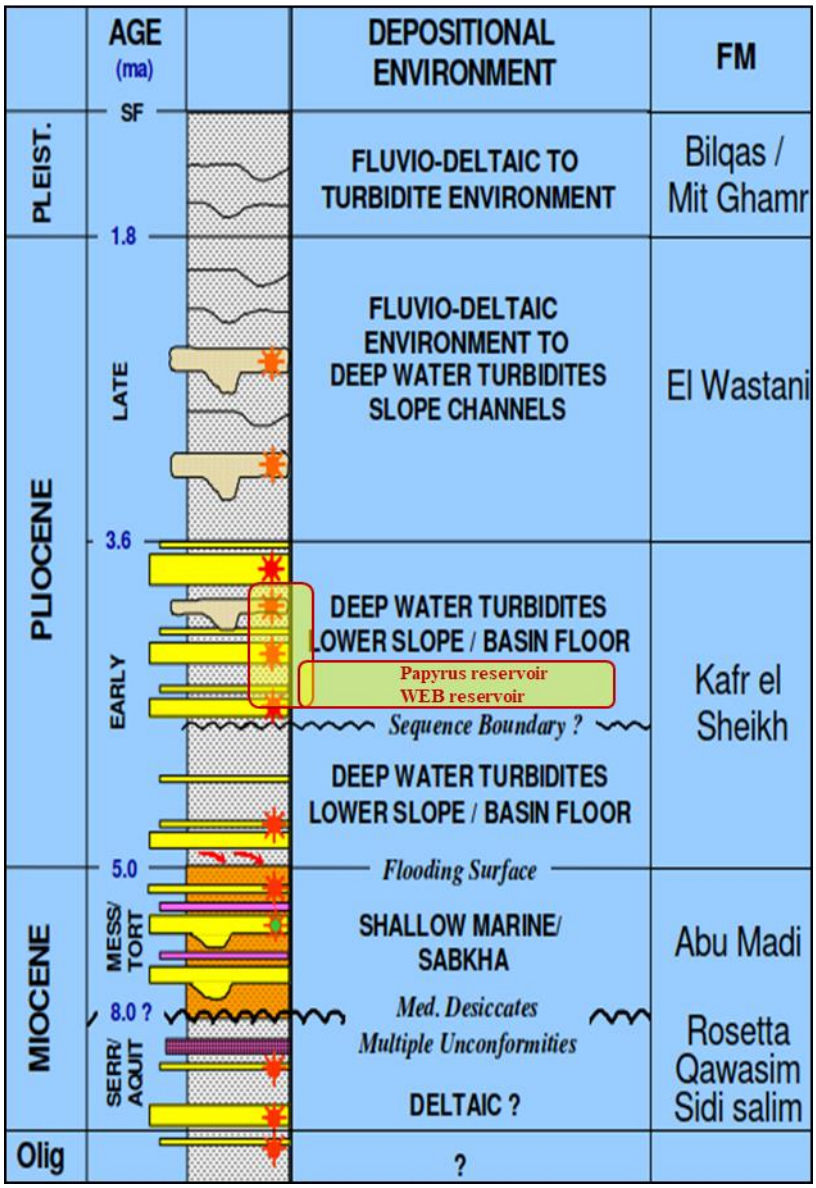

Fig.3. Chronostratigraphic chart showing the depositional environment of the study area's Miocene, Pliocene, and Pleistocene ages showing the stratigraphic setting of WEB and Papyrus reservoirs. (after Samuel et al. 2003) [8].

Data And Methodes

The 3 wells in the study area were WEB-1, Papyrus-1, and Bamboo-1, with variable quality and quantity data. The area was penetrated in 2008 with a water depth of 19.2 m below sea level at the well location. WEB-1 well targeted the Pliocene sediment of Kafr El Sheikh FM, it reached the total depth at 2335 mTVDss, Bamboo-1 was drilled to test the possible distal facies of turbidities targeted by the WEB-1 well in the WEB reservoir in the Kafr El-Sheikh formation, which is 3.7 km away from the WEB axis. Papyrus-1 well, targeted another reservoir in the Pliocene turbidities channels in the Kafr El-Sheikh formation. This well is located 3 km from the WEB-1 well on the same horst to the South of the Rosetta fault, but another Pliocene turbidities system to appraise the reservoir presence in the Papyrus channel, quality, and hydrocarbon potential of NW-SE trending Pliocene turbidities channel system; it reached the total depth at 1990mTVDss. A complete set of logs is available for the WEB-1 and Papyrus-1 wells plus Pressure sample data, while Bamboo-1 well suffered from some lack of data due to technical problems during drilling. The formation tops were defined using the bio-stratigraphical reports. All the work is done with Schlumberger Tech-Log software 2019 as follows:

Petrophysical and logging analysis

At first, we merge and splice the well logs data entry to deduct the best quality for the logs. Kafr El-Sheikh Formation is divided into various zones in every well of the study area based on the petrophysical properties and logged interval (nine zones in the WEB-1 well, four zones in the Papyrus-1 well, and four zones in the Bamboo-1 well).

Formation temperature

The temperature gradient module is used to create a continuous temperature curve. The temperature values may affect obtaining the required value of water resistivity (RW). The temperature curve is calculated either by entering a temperature gradient or by entering temperatures at fixed points (top log interval and bottom log interval) and the program extrapolates between them in WEB-1 and Papyrus-1 wells.

Water resistivity (R_w)

Several methods can be used to determine the formation of water resistivity, such as:

- Porosity resistivity cross-plots (Pickett's plot).
- Apparent water resistivity log (R_{wa}),
    - Direct laboratory measurements of formation testing water samples.
    - From water salinity value by using the charts.
    - From the Self Potential log (SP), create a continuous R_w curve.
    - From the resistivity log using Archie's equation.

In this study, the water resistivity is obtained from the Porosity-Resistivity cross-plots (Pickett's plot), which are developed by plotting porosity values with the unflushed zone (Deep) resistivity [9].

The salinity of the water in the unflushed zone

The water salinity is determined by using the resistivity of the NaCl water solution chart [10]. It is necessary to know the water resistance and temperature in this range to draw the salinity curve accurately.

Temperature and salinity parameters

The Formation temperature as input curve, Mud filtrated sample temperature, the resistivity of mud filtrated, and the salinity of the water in the unflushed zone, by knowing the mud weight for every zone and by determination of the average porosity of every zone, the main output will be water resistivity curve.

Shale Volume (V_{sh})

The clay material often referred to as "shale" may be distributed in sand formations in three forms: laminated, structural, and dispersed, [11]. The calculation of the Shale volume could be fulfilled from multiple clay indicators, either from Single or double curves indicators, e.g., Gamma-ray (GR), spontaneous potential (SP), Neutron, and deep Resistivity responses (RESD), alternatively double curves (e.g., sonic/neutron, Neutron/density, and sonic/density) curves.

Determining shale volume (V_{sh}) is crucial for reservoir rock analysis.

1- V_{sh} from the gamma-ray log as a single curve indicator:

Gamma-ray log principally due to its sensitive response to the radioactive materials normally concentrated in the shaly rocks.

The input parameters for calculating (V_{sh}) from the gamma-ray curve are GR_{clean}, GR_{shale}, and Gamma-ray $_{log}$.

$$V_{sh} = (GR_{log} - GR_{clean}) / (GR_{shale} - GR_{clean}) \quad (1)$$

2- Vsh from neutron-density logs as double curves indicators:

Can be determined in this work by using the equation [12]:

$$V_{sh} = \frac{(Den_{clean.2} - Den_{clean.1}) \times (Neu - Neu_{clean.1}) - (Den - Den_{clean.1}) \times (Neu_{clean.2} - Neu_{clean.1})}{(Den_{clean.2} - Den_{clean.1}) \times (Neu_{clay} - Neu_{clean.1}) - (Den_{clay} - Den_{clean.1}) \times (Neu_{clean.2} - Neu_{clean.1})} \quad (2)$$

Where; $Den_{clean.1}$ & $Neu_{clean.1}$, and $Den_{clean.2}$ & $Neu_{clean.2}$ are the density and neutron values for the two ends of the clean line.

Porosity determination (φ):

Total porosity (ΦT)

Total porosity can be determined by combining the readings of two porosity logs, such

as the density and neutron, as implemented in the WEB-1 well and Papyrus-1 well. Formation porosity can be determined from the density-neutron combination through the following equation [11]:

$$\phi_T = \sqrt{\frac{\Phi_{Nc}^2 + \Phi_{Dc}^2}{2.65}} \quad [\%] \quad (3)$$

The total porosity can be derived from the sonic log. Determining the total porosity in the shale-free formations or clean zones using sonic log data depends on the following formula [13], as applied in the Bamboo-1 well. Where; sonic-derived porosity (ΦS) is calculated as follows:

$$\phi S = \left(\frac{(\Delta T_{log} - \Delta T_{ma})}{(\Delta T_f - \Delta T_{ma})} \right) [\%] \quad (4)$$

Where; ΔT_{log}: is the interval transit time of the formation, ΔT_{ma}: is the interval transit time of the matrix, and Δ_{Tf}: is the interval transit time of the fluid in the well bore.

The inputs in the effective porosity and saturation step include neutron, density (WEB-1 and Papyrus-1), Sonic (Bamboo-1 well), the volume of shale, true or deep resistivity, formation water resistivity curve (RES_UWAT), formation temperature, Also determine the hydrocarbon density value equal 0.3 g/cm^3 and by applying Indonesian equation:

Effective porosity and saturation:

$$SW_{Indonesia} = \left\{ \frac{\sqrt{\frac{1}{Rt}}}{\left(\frac{Vsh^{(1-0.5Vsh)}}{\sqrt{Rsh}} \right) + \sqrt{\frac{\phi_e^m}{a.Rw}}} \right\}^{(2/n)} \quad (5)$$

In the present study, effective porosity was used to calculate water saturation. The effective porosity depends on the degree of connection between the rock pores with each other, forming channels to facilitate the path of fluids through the lithological contents. Two ways to calculate the effective porosity [11]:

The first way is using the following general equation:

$$\phi E_1=\phi T*(1-V_{sh}) \quad (6)$$

Where ΦT is total porosity and V_{sh} is the volume of shale.

The second way is the application of the empirical relation:

$$\Phi E_2= (2\Phi Nc +7\Phi Dc) / 2 \quad (7)$$

Where; ΦNC and ΦDC are corrected neutron and density-derived porosities for the shale effect, respectively. The effective porosity (ΦE) could be taken as the mean value of ΦE_1 and ΦE_2.

The Indonesian equation is suitable for the study wells; due to the volume of shale in the reservoirs, more than 10% where the sandstone is described as shaly sand. As shown in the Indonesia formula, the shale resistivity has been determined. Due to the absence of core data for the wells WEB-1 and Bamboo-1, the common standard petrophysical parameters used from the offset and adjacent wells to the WEB area for the WEB-1 and Bamboo-1 are a= 1,m= 2,n= 2. While a= 1, m= 1.79, and n= 1.93 for (Papyrus-1 well) from core data (Internal Core Data Report).

Lithology computation

This method aims to determine quartz volume using the volume of shale, effective porosity, water saturation, and density curves. Finally, by applying the difference cutoffs for the studied wells, we can get the final petrophysical results.

Pressure tests/ modular dynamic formation tester (MDT)

A modular dynamic formation tester is used to confirm the interpretation of the logs, determine the formation pressure, and get the true formation fluid samples. By plotting the pressure points against depth, we calculate the gas-water, oil-water, and gas-oil contacts.

Cross-plotting relationships (lithological identification)

Cross-plotting relationships have been constructed to help identify the distribution behavior of the well-logging deduced parameters, particularly the porosity. Many cross plots (Neutron-density, Sonic-density, Sonic-neutron, and M-N) facilitate the qualitative interpretation of some log responses, e.g., deducing the mineral constituents and lithology in the studied rock units. The following describes one type of cross plot (Neutron-Density) constructed for the examined formations from the studied wells.

RESULTS AND DISCUSSION

Petrophysical Results

Formation temperature

The temperature readings used in the WEB-1 well were 10°C @ 19.2 m TVDSS and 77.28°C @ 2123.3 m TVDSS (Fig. 4a). On the other hand, the temperature readings used in Papyrus-1 well were 66.52°C @ 1802.56 m TVDSS and 77.28°C @ 1962.18 m TVDSS (Fig. 4b). The temperature values are unavailable to obtain temperature values for Bamboo-1well.

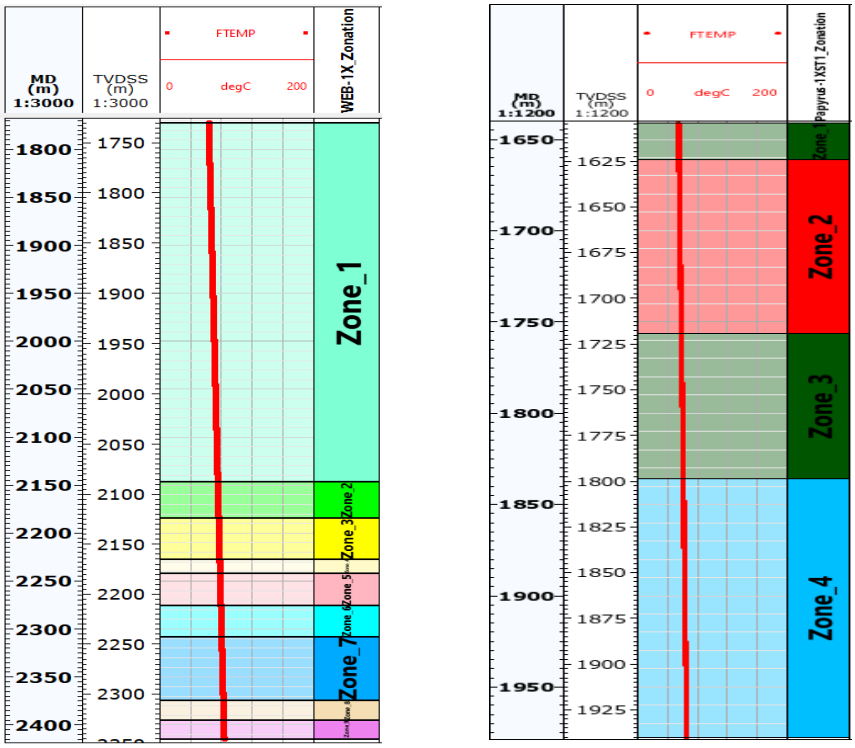

Figure (4): Temperature gradient curve of WEB-1 well (a), Temperature gradient curve of Papyrus-1 well (b) in Kafr El Sheikh Formation zones.

Water resistivity (R_w)

The nearest selected clean water-bearing sandstone zone to the pay zone is shown in Figure (5) for the WEB-1 well. In the Kafr El-Sheikh formation (Pliocene Age), for the WEB-1 well, the water resistivity value is 0.05 Ohm.m @ 2230.5 m., while the water resistivity in Bamboo-1 well value is 0.03 Ohm.m @ 1672 m (Fig. 6)**,** while the Papyrus-1 well, the water resistivity value is 0.058 Ohm.m @ 2230.5 m.1974 m (Fig. 7).

Shale Volume (V_{sh})

Shale volume is calculated as the arithmetic mean value from double curves indicator (Neutron / Density) and single curve indicator (Gamma-ray) for WEB-1 well (Fig. 8) and Papyrus-1 well (Fig. 9)**,** while the Bamboo-1 well we used a single curve indicator (Gamma-ray) to calculate the shale volume due to the lack of data (Fig. 10)**.**

Effective porosity and saturation

The calculated effective porosity and fluid saturation in the Kafr El-Sheikh Formation

focusing on the pay zone for WEB-1, Bamboo-1, and -1 Papyrus-1 wells by applying the main output result (Fig. 11, 12,and 13)**.**

Lithology computation

This method aims to determine quartz volume using the volume of shale, effective porosity, water saturation, and density curves of WEB-1 and Papyrus-1 wells in (Figs 14 and 15) respectively, while lithology computation is absent in Bamboo-1 well due to the absence of density log.

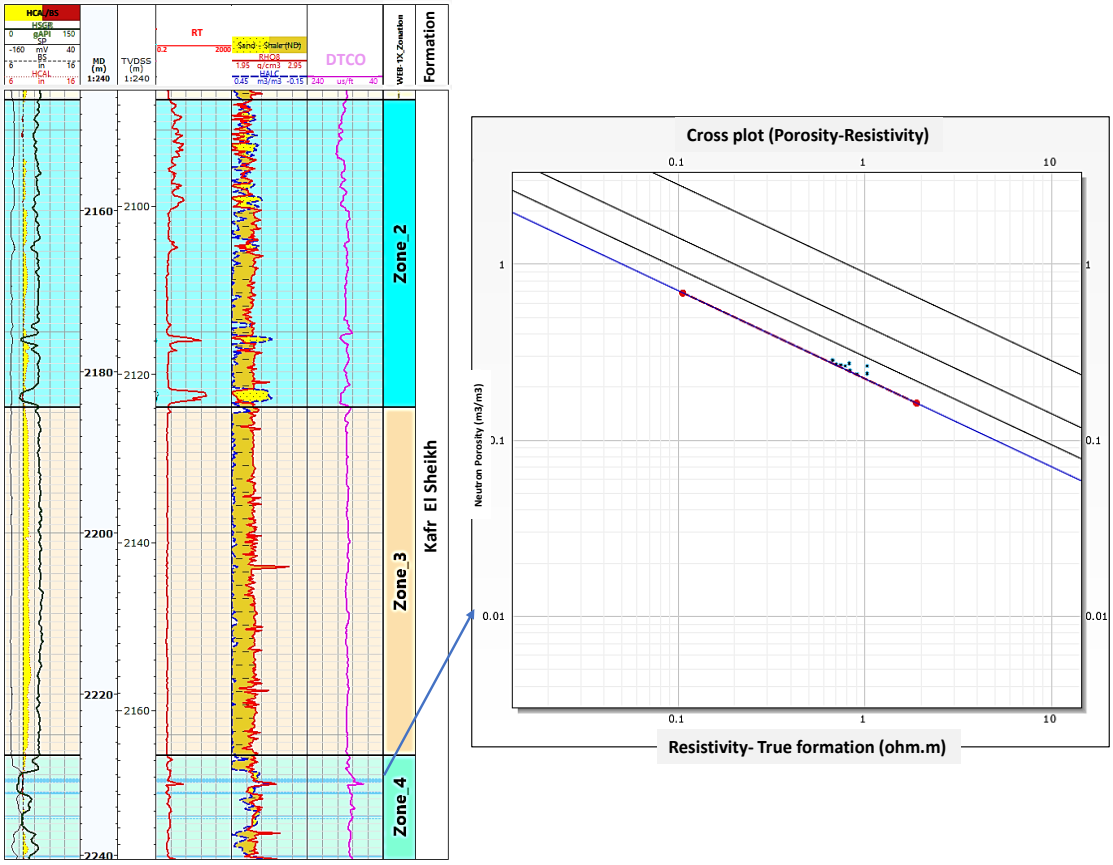

Figure (5): WEB-1well Resistivity versus porosity Pickett plot.

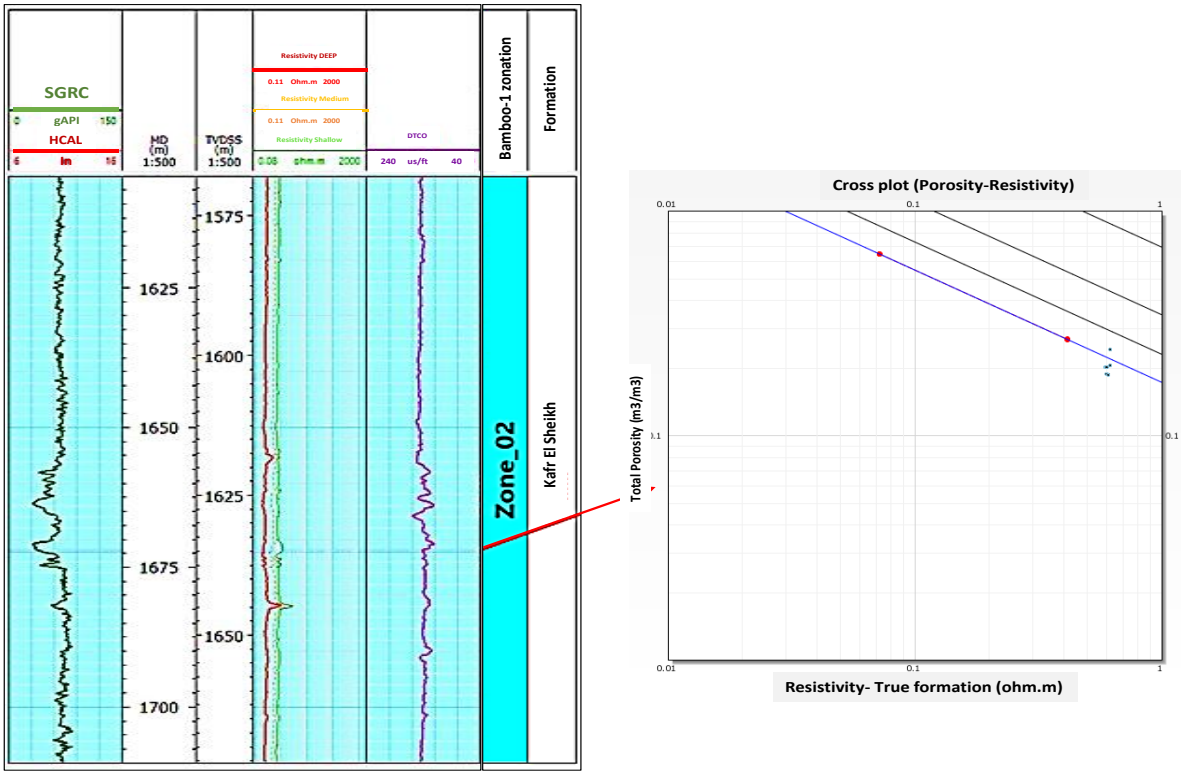

Figure (6): Bamboo-1well Resistivity versus porosity Pickett plot.

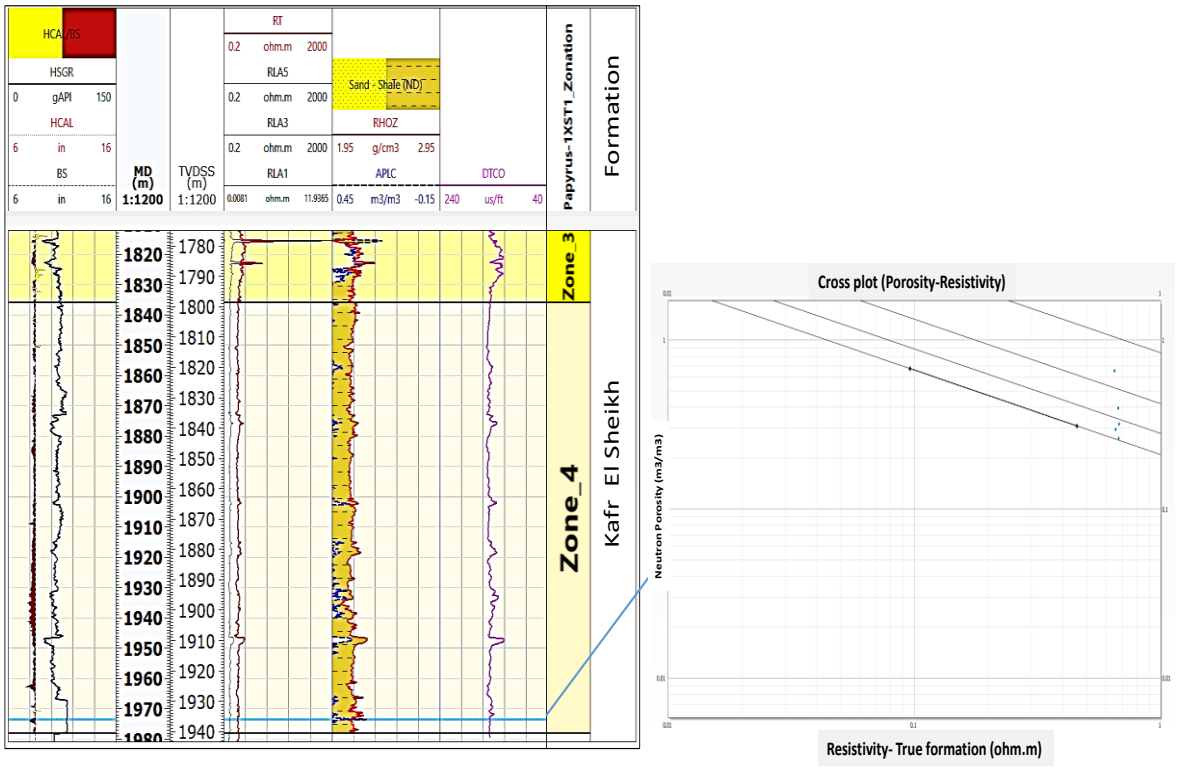

Figure (7): Papyus-1well Resistivity versus porosity Pickett plot.

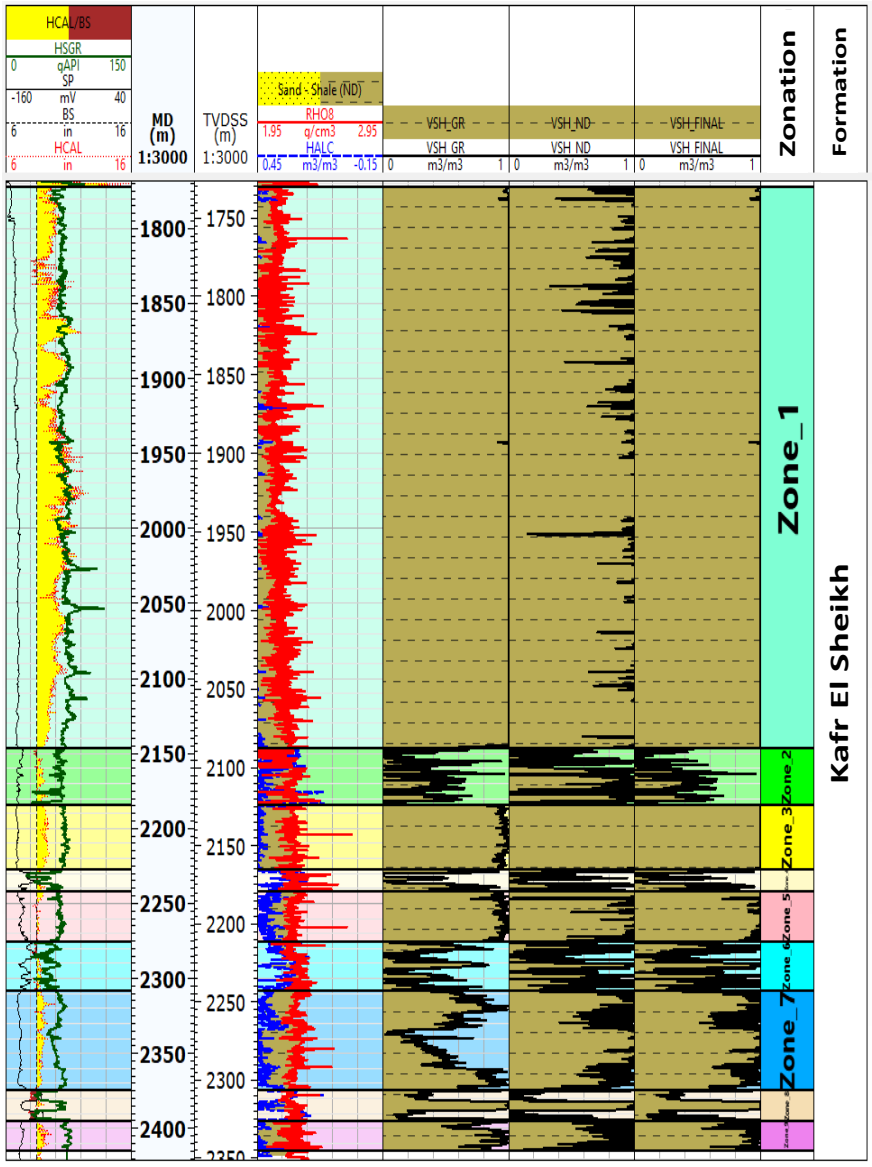

Figure (8): Presentation of the calculated volume of the shale in the Kafr El-Sheikh Formation, WEB-1 well.

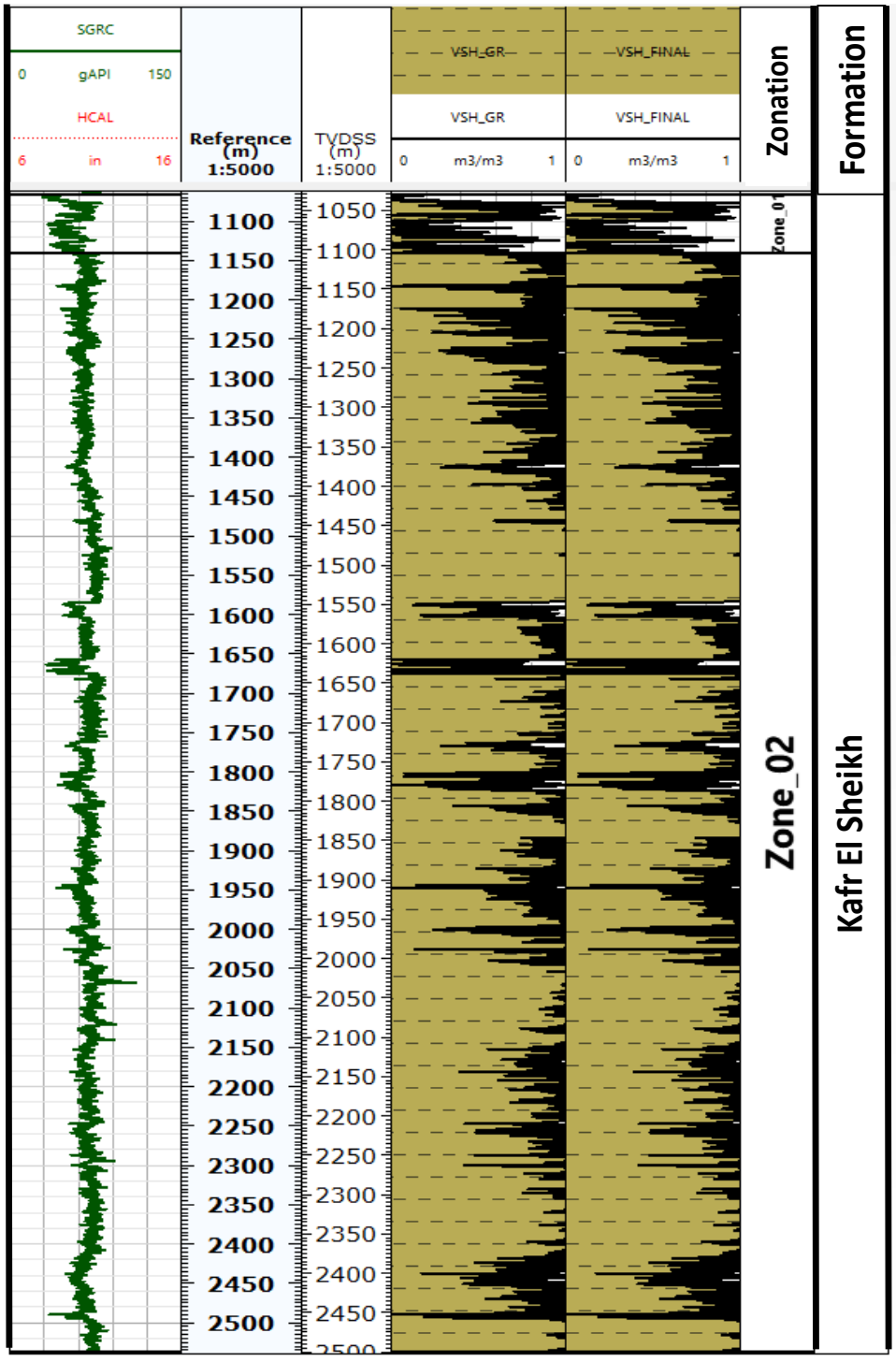

Figure (9): Presentation of the calculated volume of the shale in the Kafr El-Sheikh Formation, Bamboo-1 well.

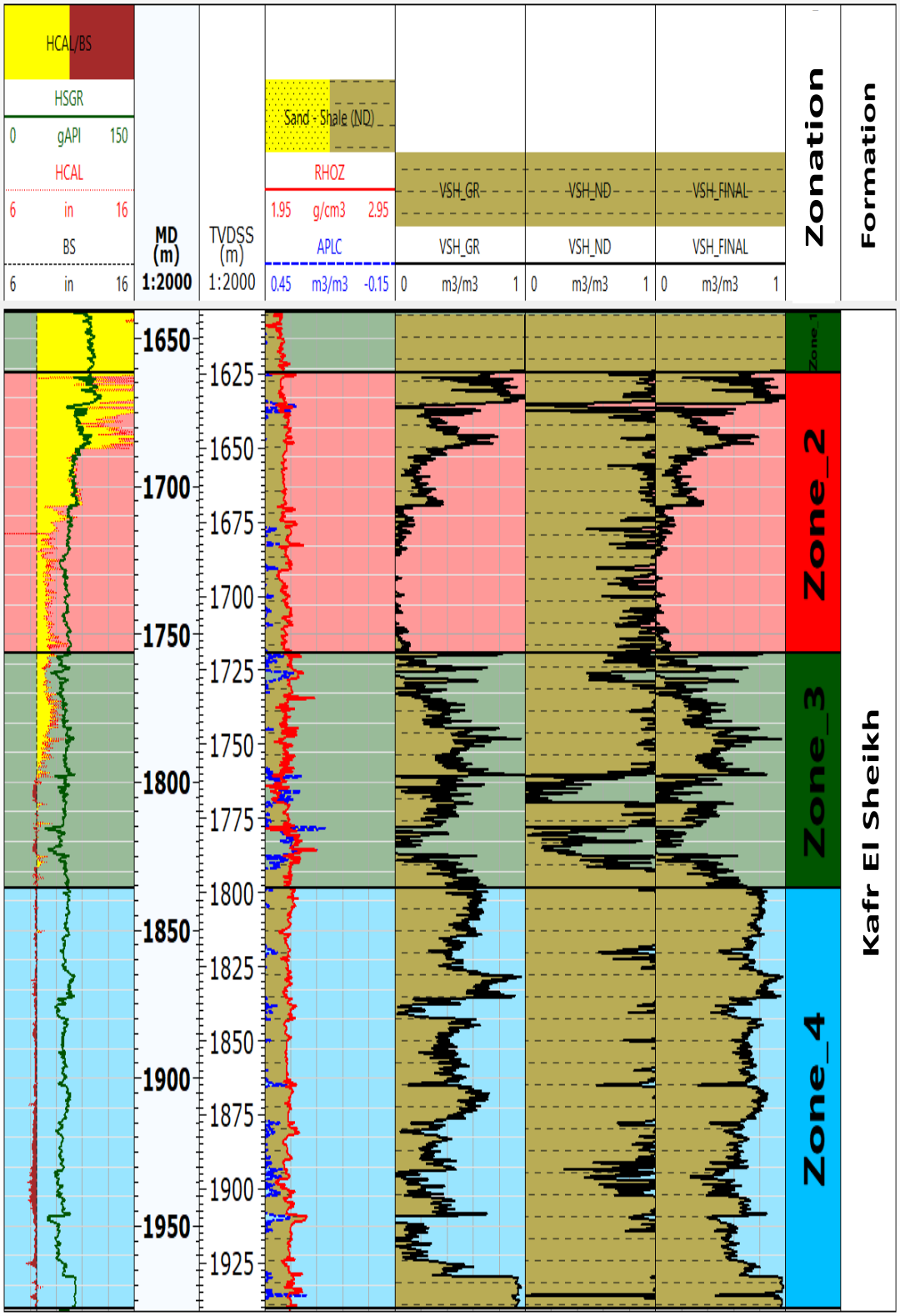

Figure (10): Presentation of the calculated volume of the shale in the Kafr El-Sheikh Formation, Papyrus-1 well.

Figure (11): Presentation of the calculated effective porosity and fluid saturation in the Kafr El-Sheikh Formation focusing on the pay zone, WEB -1well.

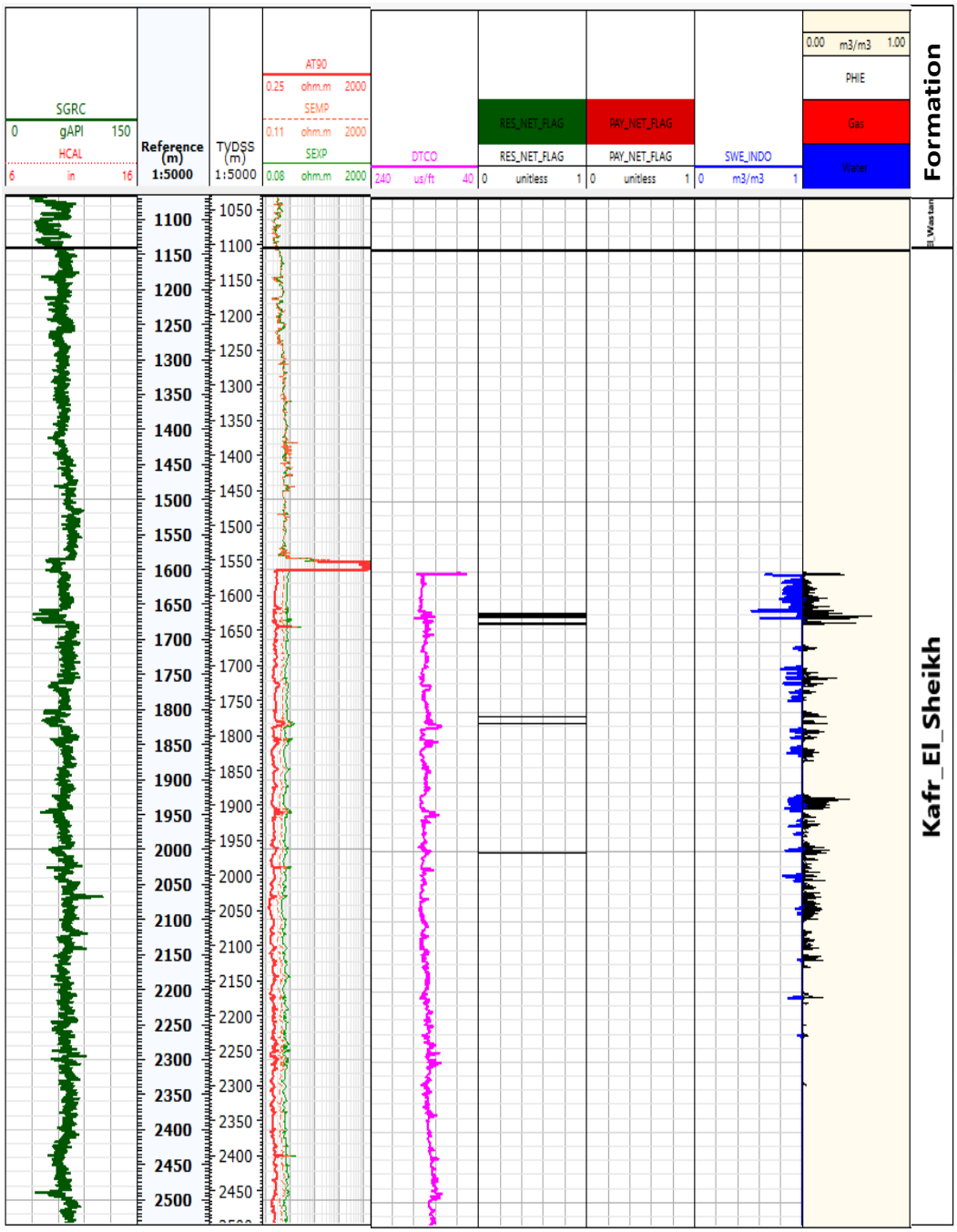

Figure (12): Presentation of the calculated effective porosity and fluid saturation in the Kafr El-Sheikh formation focusing on the pay zone, Bamboo -1well.

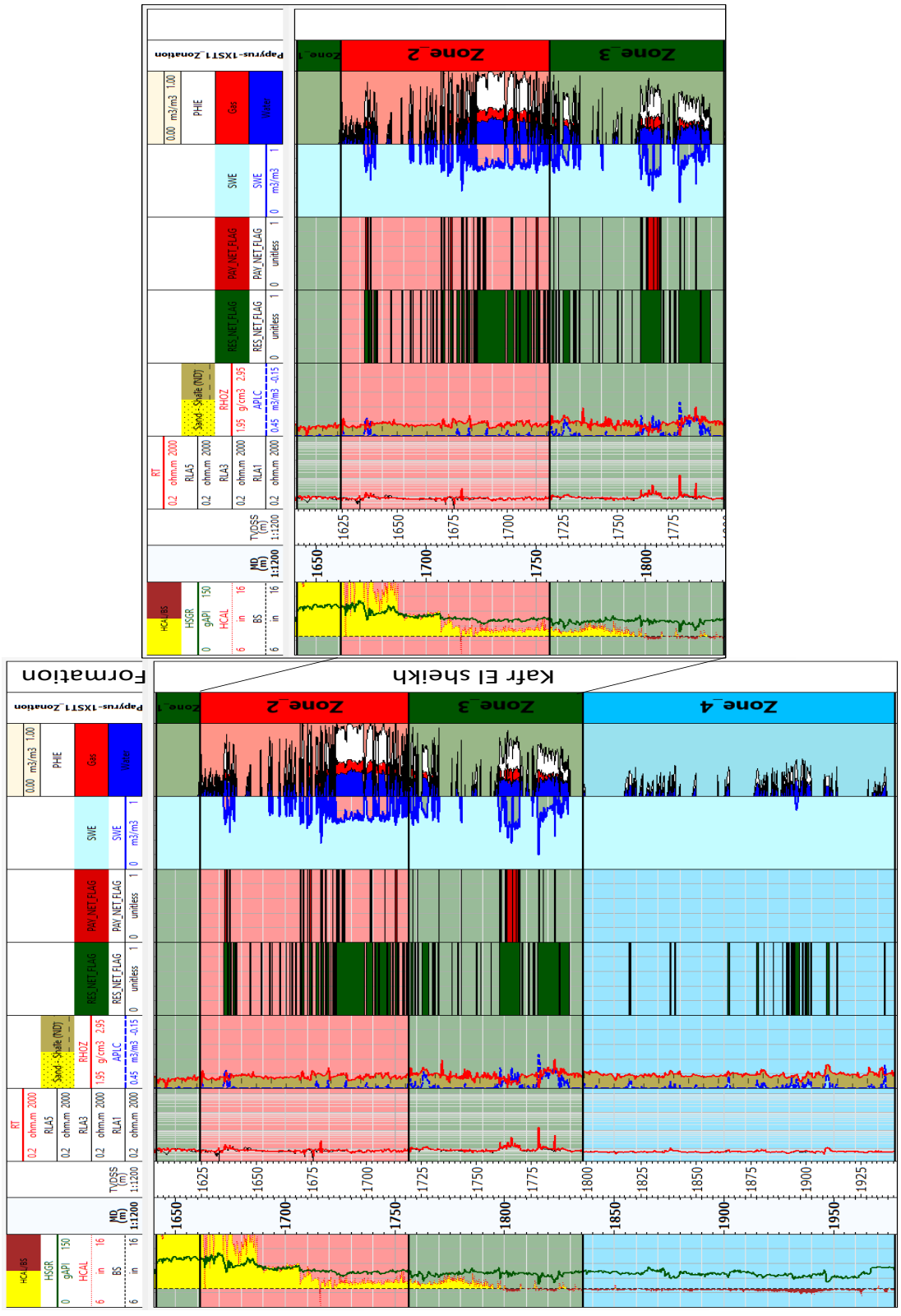

Figure (13): Presentation of the calculated effective porosity and fluid saturation in Kafr El-Sheikh formation, Papyrus-1well.

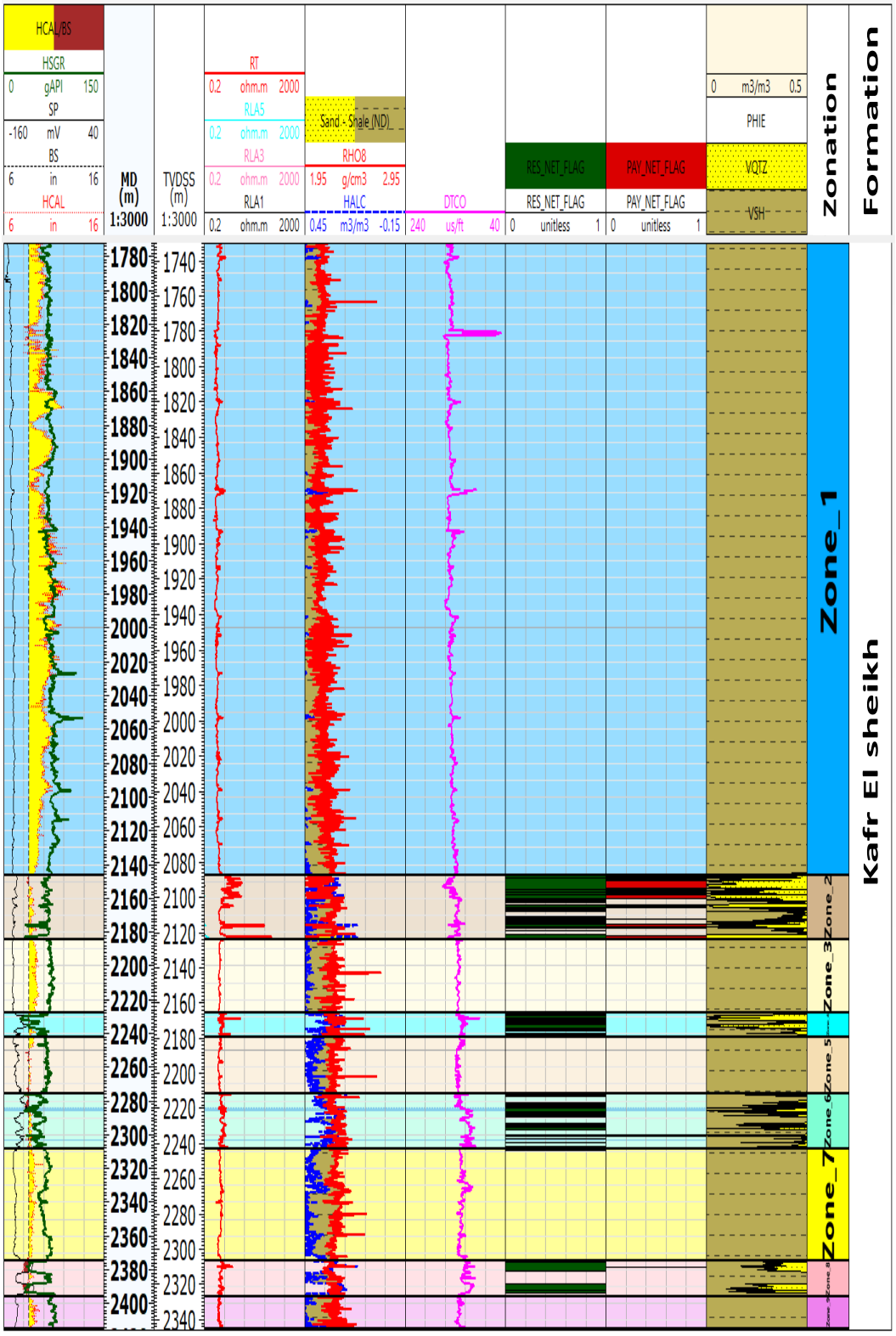

Figure (14): WEB-1 well, Lithology interpretation of Kafr El-Sheikh FM.

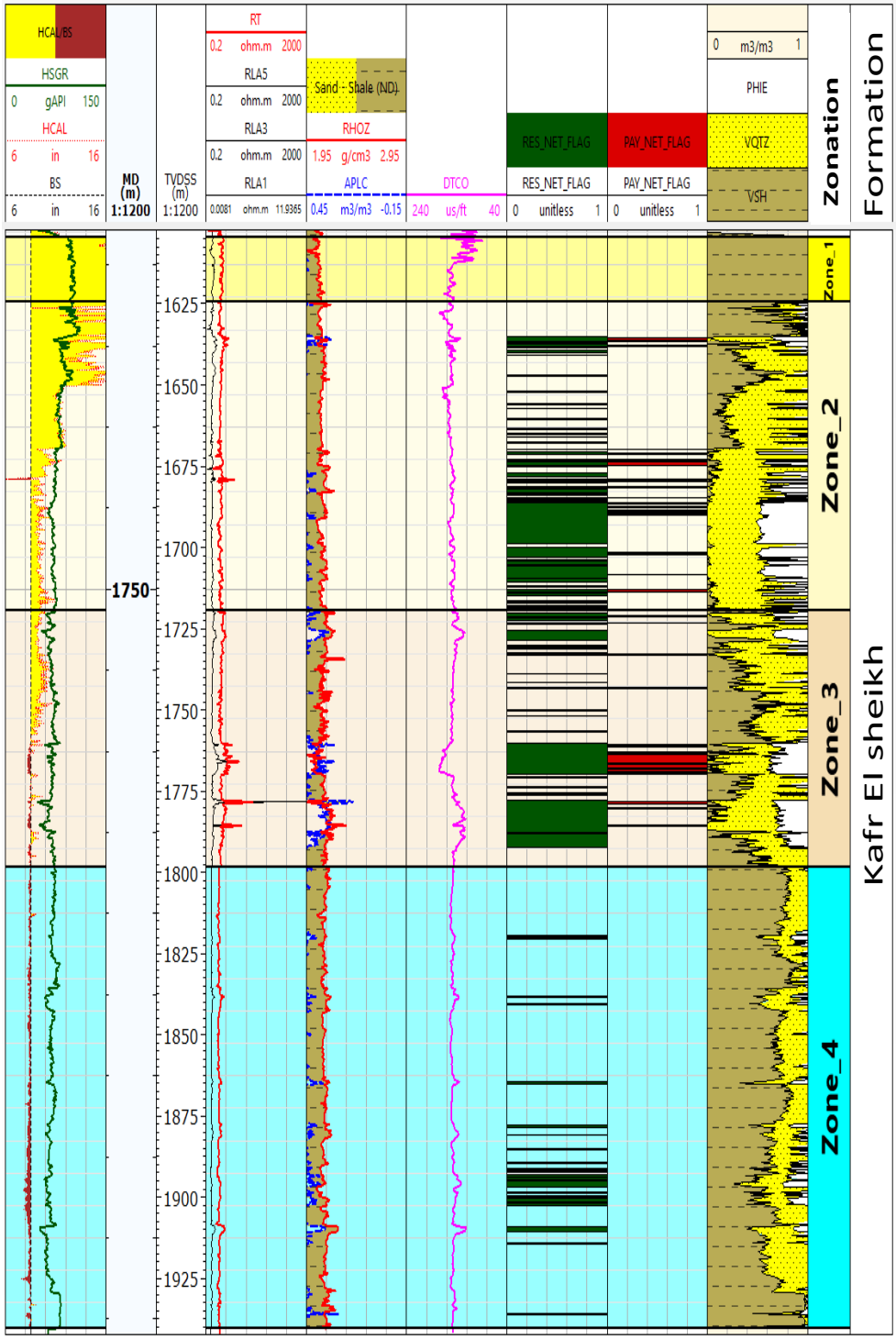

Figure (15): Papyrus-1 well, Lithology interpretation of the El-Sheikh FM.

Petrophysical evaluation

The final petrophysical results conclude that the Web-1 well reflected hydrocarbon in three zones with an average net pay of around 16.8 m; only one is important (zone-2), and the other zones (zone-6 and zone-8) from the hydrocarbon point of view is not interesting. Papyrus-1 well contains hydrocarbon in two important zones (zone-2 and zone-3), with an average net pay of around 15.14m.On the other hand, Bamboo-1 well does not contain any hydrocarbon zone as the well penetrate the distal facies of the WEB channel/levees complex and failed to find any reservoir extension (Table 1).

Table (1): The values of petrophysical parametres for Kafr El-Sheikh formation results in WEB-1, Papyrus-1,and Bamboo-1 wells in West El-Burullus field, Offshore, Nile Delta, Egypt.

Zones	Top	Bottom	Gross (m)	Net Pay (m)	Vsh,(%)	PHIE,(%)	Sw,(%)
WEB-1 well							
Zone-1	1729.6	2087.3	357.7	-	-	-	-
Zone-2	2087.3	2123.9	36.5	15.6	0.0	0.3	0.4
Zone-3	2123.9	2165.4	41.5	-	-	-	-
Zone-4	2165.4	2178.9	13.5	-	-	-	-
Zone-5	2178.9	2211.2	32.3	-	-	-	-
Zone-6	2211.2	2242.6	31.5	0.9	0.0	0.3	0.6
Zone-7	2242.6	2306.2	63.6	-	-	-	-
Zone-8	2306.2	2326.4	20.1	0.3	0.2	0.2	0.6
Zone-9	2326.4	2344.8	18.4	-	-	-	-
Papyrus-1 well							
Zone-1	1604.2	1624.3	20.1	-	-	-	-
Zone-2	1624.3	1719.1	1719.1	5.6	0.0	0.5	0.6
Zone-3	1719.1	1798.4	79.4	8.5	0.1	0.4	0.6
Zone-4	1798.4	1940.4	0.0	-	-	-	-
Bamboo-1 well							
Zone-1	1029.3	1103.6	74.3	-	-	-	-
Zone-2	1103.6	2499.1	1395.5	-	-	-	-
Zone-3	2499.1	3161.4	662.3	-	-	-	-
Zone-4	3161.4	3635.5	474.1	-	-	-	-

The promised two wells (WEB-1 and Papyrus-1) were tested by Pressure tests or Modular dynamic formation tester (MDT) and We obtained the Gas-Water, Oil-water, and gas- Oil contacts by plotting the pressure points against depth. To evaluate the pressure gradients and fluid type of the gas shows and subsequent log evaluation, 17 good pressure readings were taken of WEB-1 well in Kafr El-Sheikh Formation between 2088.65 m TVDSS (6852.97 ft) and 2321.88 m TVDSS (7618.17 ft) (Table 2). The intersection of the water and gas gradients at 2149 m TVDSS in the WEB-1 well reservoir identifies the gas-water contact depth (Fig. 16a). It's clear from the MDT plot that the water gradient values range from 0.427 psi/ft to 0.448 psi/ft, and the gas gradient value is 0.119 psi/ft, which is likely rich thermogenic gas which may be Miocene sourced and migrated upward through the major faults such as the Rashid fault and its successive faults.

Through the Papyrus-1 well 10 good pressure readings were taken in the Kafr El-Sheikh Formation reservoir between 1761.61m TVDSS (5779.84 ft) and 1893.96m TVDSS (6212.18 ft) (Table 2). The MDT of Papyrus-1 well shows that the gas is down (Fig. 16b).

Table (2): The Pressure tests values or Modular dynamic formation tester values (MDT) for Kafr El-Sheikh formation in WEB-1, and Papyrus-1wells of West El-Burullus gas field, Offshore Nile Delta, Egypt.

Well	Formation Pressure (psi/ft)	Depth TVD_{SS} (ft)	Depth TVD_{SS} (m)	Zones
WEB-1 well	4940.46	6852.97	2088.68	Zone 1
	4941.73	6868.04	2093.28	
	4942.62	6876.52	2095.86	
	4942.88	6879.66	2096.82	
	4943.67	6884.37	2098.25	
	4944.18	6889.08	2099.69	
	4945.61	6907.92	2105.43	
	4951.2	6943.99	2116.43	
	4991.12	7117.14	2169.2	Zone 2
	4996.38	7129.75	2173.04	
	4998.09	7132.9	2174	
	5067.27	7290.51	2222.04	Zone 3
	5087.73	7336.23	2235.97	
	5188.01	7577.24	2309.43	

	5192.21	7586.68	2312.31	
	5205.54	7618.17	2321.91	
Papyrus-1 well	4103.77	5778.07	1761.61	Zone 1
	4106.01	5794.15	1766.51	
	4105.77	5799.69	1768.2	
	4106.03	5800.35	1768.4	
	4107.62	5803.62	1769.4	
	4109.13	5835.07	1778.98	
	4109.97	5835.39	1779.08	
	4109.23	5836.38	1779.38	
	4378.64	6205.95	1892.06	**Zone 2**
	4379.96	6212.18	1893.96	**Condensate**

Cross-plot relationships (lithological identification)

The measurements of the neutron, density and sonic logs depend on porosity, formation lithology, the pore fluid, and some instances, the geometry of the pore structure [14]. Neutron-Density cross-plots are used efficiently to distinguish between sand, silt, and shale units. In each well, the neutron porosity VS. Bulk density cross plots is also studied and plotted along the abscissa and ordinate, respectively. The shale units with high neutron porosity and high-density values lie on the right side of the cross plot; in contrast, the clean sand units have lower neutron porosity and density values and thus lie on the left side. Figures (17, 18, and 19) show the Neutron-Density plots for all studied wells (WEB-1, Papyrus-1 and Bamboo-1 wells). It is evident from the cross plots that show the presence of sand-shale mixed lithology in all three wells. The gas effect pulled up the plotted data to the upper left-hand side of the plot in the WEB-1 and Papyrus-1 wells, respectively, and the majority of points plotted to the below right-hand side of the plot because of the shale effect, while Bamboo-1 well cross plot showing absence of any gas effect.

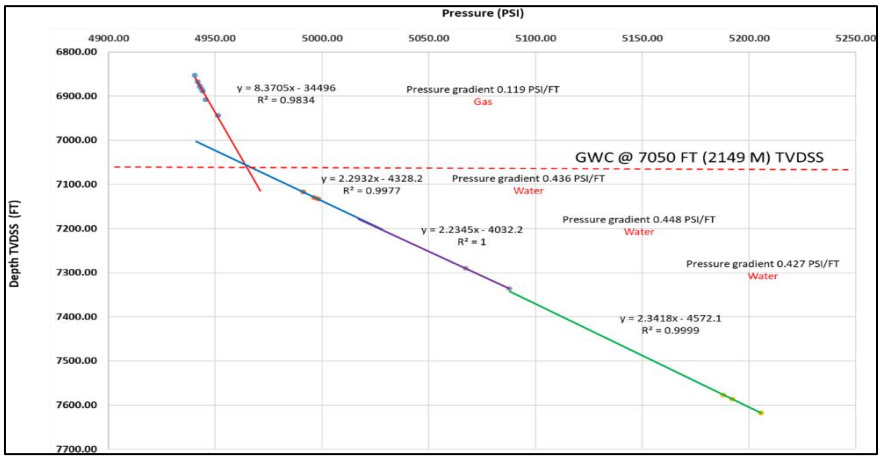

(a

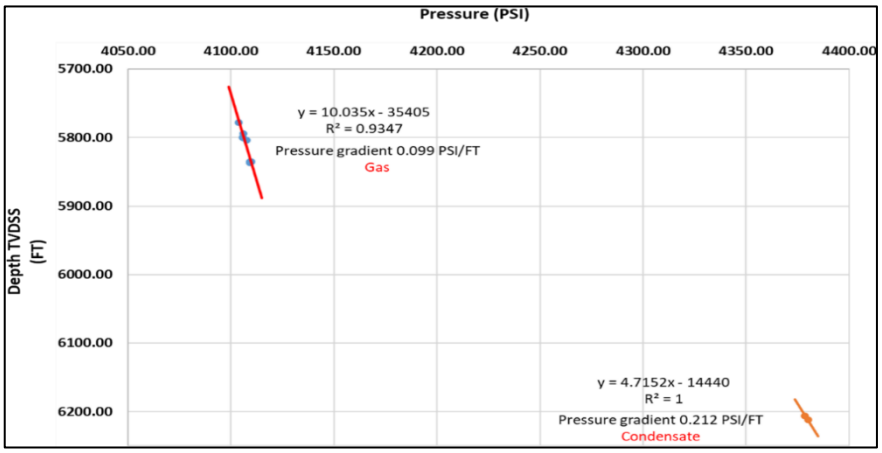

(b

Figure 16: WEB-1 and Papyrus-1 wells MDT plotting for Kafr El-Sheikh Formation reservoir.

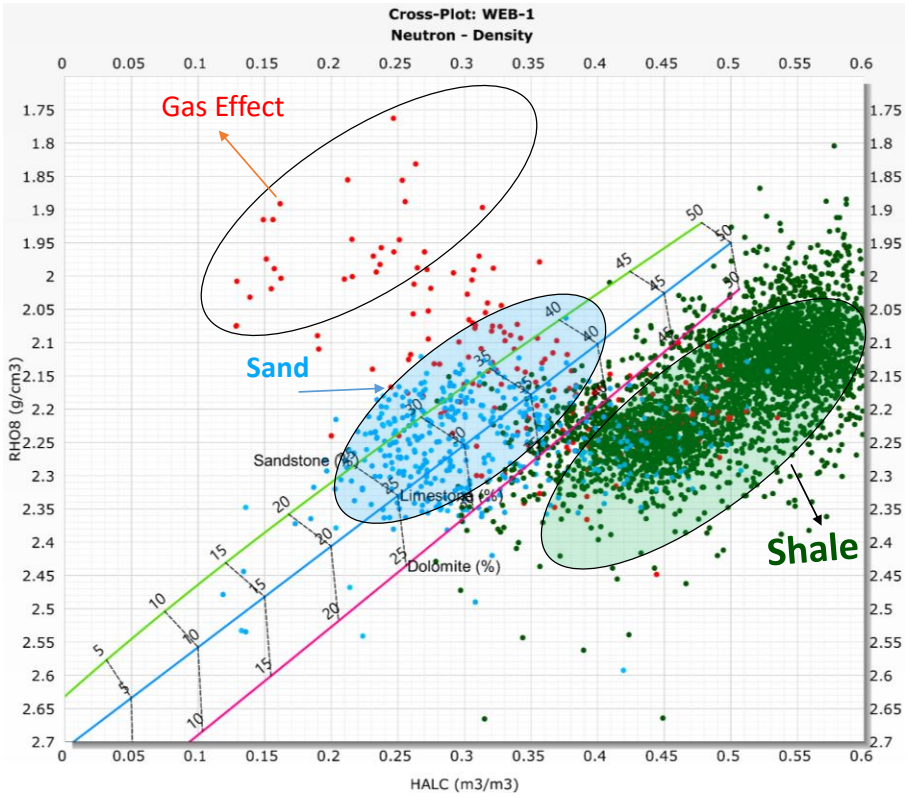

Figure 17: WEB-1 well Neutron-Density cross plot for Kafr El-Sheikh FM.

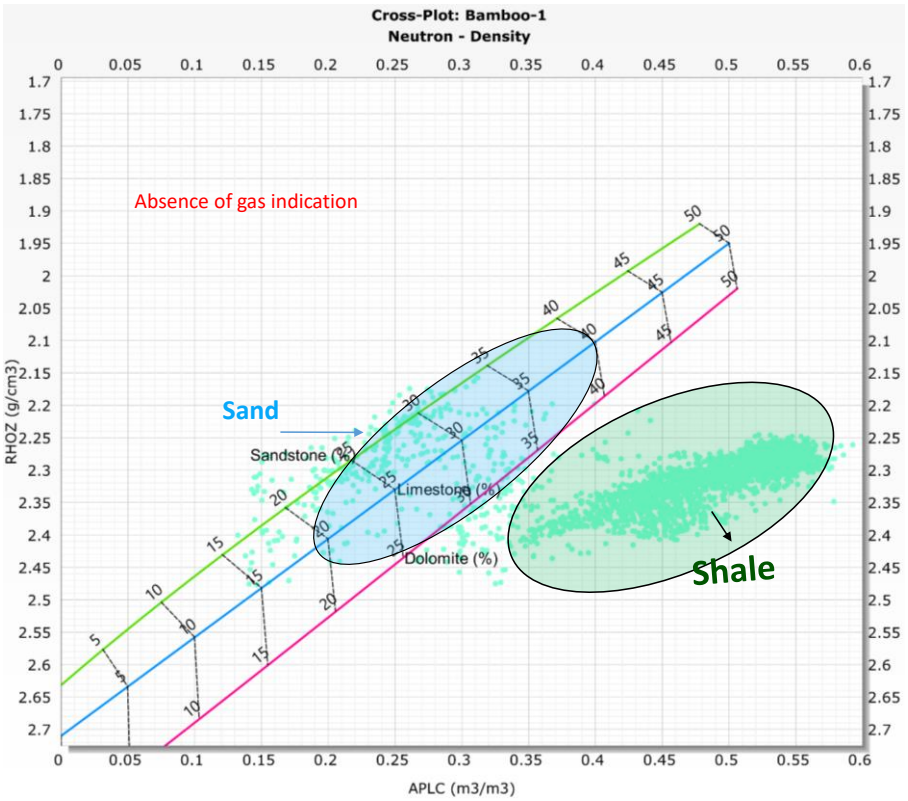

Figure 18: Bamboo-1 well Neutron-Density cross plot for Kafr El-Sheikh FM.

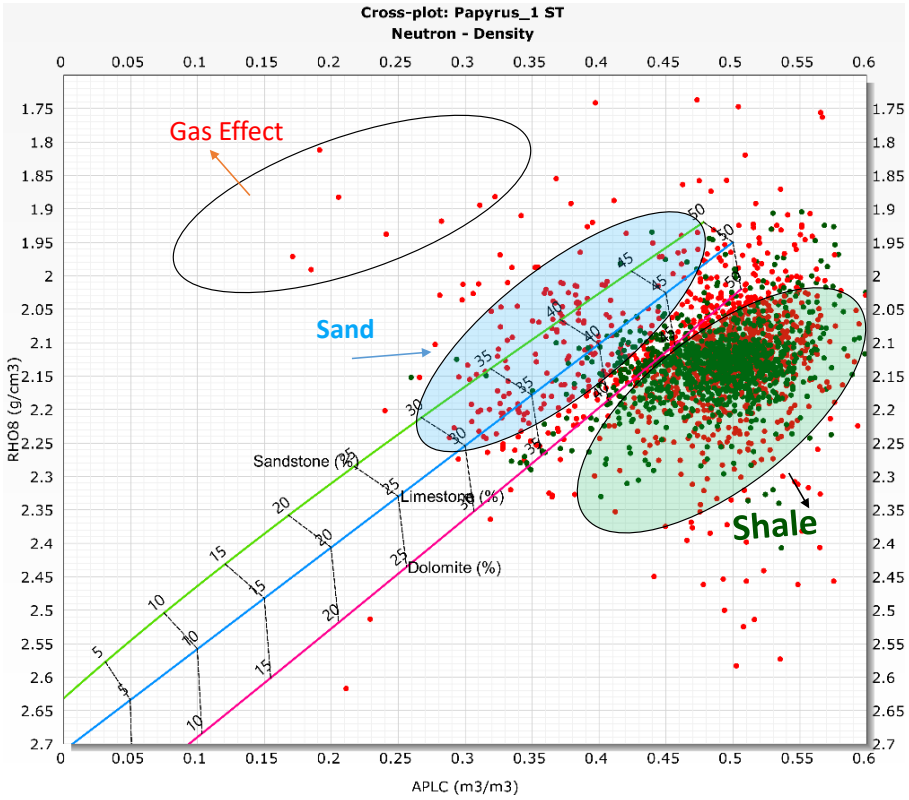

Figure 19: Papyrus-1 well Neutron-Density cross plot for Kafr El-Sheikh FM.

Conclusion

The petrophysical analysis accompanied by pressure readings and petrophysical relationships gives great reliability to geological interpretations related to wells, especially exploratory wells. Using well logging properties and integrating them with the modular dynamic formation tester (MDT), followed by Cross-plotting relationships as lithological/hydrocarbon identification that will overcome the great challenge of accurately determining the existence of hydrocarbons in turbidites and confirm the interpretation of the logs.

The results proved that the Web area contains hydrocarbon with an average net pay of around 32m in two different reservoirs Web and Papyrus respectively; On the other hand, the failure of some wells is due to entering outside the boundaries of the reservoirs by penetrating the distal facies channel/levees complex which is mainly shales and failed to find any reservoir extension. All the results are matched very well with MDT which the Gas-Water contacts the gas gradient and the type of gases determined as likely rich gas and thermogenic (may be Miocene sourced) and migrated upward through the major faults such as the Rashid fault and its successive faults. The neutron density plots for all studied wells (WEB-1 Papyrus-1 and Bamboo-1 wells). It is a shred of strong evidence from the cross plots that show the presence of sand-shale mixed lithology in all three wells. The gas effect pulled up the plotted data to the upper left-hand side of the plot in the WEB-1 well and Papyrus-1 well, and the majority of points plotted to the below right-hand side of the plot because of the shale effect, while the Bamboo-1 well cross-plot showing absence of any gas effect.

The study area requires more geological and geophysical studies to find out the limits of the reservoir extension within the study area. It also requires knowing whether there are more sediments similar to the discovered sediments, by the study of seismic surveys and the application of some advanced seismic studies for example but not limited such as spectral decomposition analysis.

REFERENCES

1. **Kellner, A.; Brink, G.J.; el Khawaga, H.:** Depositional history of the western Nile Delta, Egypt: Late Rupelian to Pleistocene. Am. Assoc. Pet. Geol. Bull. **102**, 1841–1865 (2018). https://doi.org/10.1306/02161817234

2. **Hashem, A., Rizk, R., Gaber, M., Bunt, R., Mckeen, R.:** Petroleum system analysis of southeast El Mansoura area and its implication for hydrocarbon exploration, onshore ND,

Egypt. In The Mediterranean Offshore Conference (MOC) May (2010).

3. **Bentham, P.:** Understanding crustal structure and the early opening history of the Eastern Mediterranean Basin, offshore Northern Egypt, and the Levant. In: New and Emerging Plays in the Eastern Mediterranean, 23–25th February 2011, pp. 67–68. The Geological Society, Burlington House (2011).

4. **Said, R**.: The River Nile: Geology, Hydrology, and Utilization. Pergamon Press, Oxford (1993)

5. **Abdel Aal, A.A.; el Barkooky, A.; Gerrits,M.; Meyer, H.; Schwander, M.; Zaki, H.:** Tectonic evolution of the Eastern Mediterranean Basin and its significance for hydrocarbon prospectivity in ultra-deepwater of the Nile Delta.GeoArabia 6, 363–384 (2001). https://doi.org/10.2113/geoarabia0603363.

6. **Dolson, J.C.; Boucher, P.J.; Siok, J.; Heppard, P.D.:** Key challenges to realizing full potential in an emerging giant gas province: Nile Delta/Mediterranean offshore, deepwater, Egypt. Geol. Soc. Lond.Pet. Geol. Conf. Ser. 6, 607–624 (2005). https://doi.org/10.1144/0060607.

7. **Rizzini, A.; Vezzani, F.; Cococcetta, V.; Milad, G.:** Stratigraphy and sedimentation of a Neogene—Quaternary section in the Nile Delta area (A.R.E.). Mar. Geol. **27**, 327–348 (1978). https://doi.org/10.1016/0025-3227(78)90038-5

8. **Samuel, A., Kneller, B., Raslan, S., Sharp, A., Parsons, C**.: Prolific deep-marine slope channels of the ND, Egypt. Am Assoc Pet Geol Bull. 87, pp. 541–560 (2003). https://doi.org/10.1306/1105021094

9. **Asquith, G. B., and Gibson, C. R., 1982**. Basic well-log analysis for geologists. Tulsa: American Association of Petroleum Geologists. Vol. 3.https://doi.org/10.1306/Mth3425

10. **Schlumberger. 2009,** Log Interpretation Charts 2009 Editions.

11. **Schlumberger. 1972.** The essentials of log interpretation practice. Serv. techniques. Schlumberger, France, pp, 45-67.

12. **Schlumberger. (2008).** IP- Interactive Petrophysics V-3.5, Manual.

13. **Wyllie, M. R. J., Gregory, A. R., and Gardner, G. H. F. 1958.** An experimental investigation of factors affecting elastic wave velocities in porous media. Geophysics, Vol.23, No.3, 459-493. https://doi.org/10.1190/1.1438493

14. **Schlumberger. (1987).** Log interpretation: principals and applications. Housten, Schlumberger, France, pp, 45-67.